

A Novel Technique to the Computation of Cutoff Wavenumbers in Eccentric Coaxial Waveguides

Johnes R. Gonçalves^{*(1)} and Guilherme S. Rosa⁽¹⁾

(1) Pontifical Catholic University of Rio de Janeiro, Rio de Janeiro, RJ 22451-900, Brazil

Abstract

This paper introduces a novel method for the calculation of cutoff wavenumbers of transverse electric (TE) and transverse magnetic (TM) modes in eccentric coaxial waveguides based on a combination of the conformal mapping and perturbation techniques. Different from commonly used approaches, that are grounded on complicated determinantal characteristic equations resulting from a translational addition theorem, our method relies on a direct solution for a Helmholtz equation via a convergent power series.

1 Introduction

In the last years, many authors have been studied and developed techniques for solving the problem of eccentric coaxial waveguides and calculate the cutoff wavenumber of TE and TM modes present in this structure. One of the first formal techniques explored was presented in [1], where the boundary-value problem was solved using a numerical point-matching method. Another method proposed in [2], solves the problem at hand by utilizing the translational Graf's addition theorem for modeling small eccentricities in coaxial waveguides. More recently, the method presented by [3] also employs an addition theorem for cylindrical functions, but in approximated fashion.

Another popular method for characterizing eccentric waveguides is based on the conformal mapping [4, 5] of the original problem into another geometry that allows a feasible boundary problem resolution. In [5], the lower and upper bounds of the cutoff frequencies were obtained by combining a conformal mapping with the Rayleigh-Ritz method. In the recent work in [6], the Helmholtz equation was analyzed in a bipolar coordinate system, and convenient approximations have allowed a solution based on the separation of variables.

In this paper, we introduce a conformal mapping to transforming the geometry of the original problem of a coaxial waveguide comprising two eccentric cylinders (see Fig. 1(a)) into an equivalent problem with two concentric boundaries (see Fig. 1(b)). As a consequence of this transformation, the medium becomes anisotropic and inhomogeneous, with electric permittivity and the magnetic permeability presenting radial (ρ) and azimuthal (ϕ) dependence. In order to find the cutoff wavenumbers, we explored the concept of cavity-material perturbations [7] in

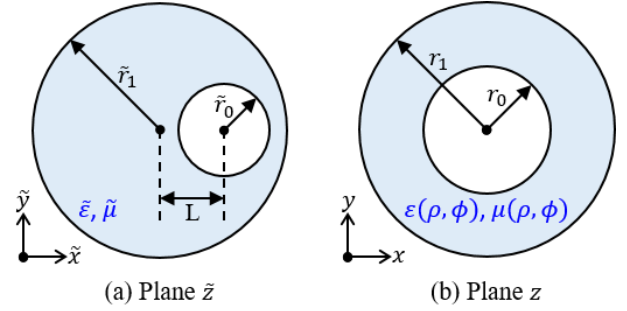


Figure 1. (a) Geometry of an eccentric coaxial waveguide. (b) Geometry of the transformed waveguide.

the transformed geometry shown in Fig. 1(b). Numerical results are presented, demonstrating the accuracy of our method when compared with the solution from finite element method (FEM).

2 Formulation Overview

2.1 Conformal Mapping

In order to solve the problem of an eccentric coaxial waveguide, let us first apply a conformal mapping to transform the geometry in Fig. 1(a) to that in Fig. 1(b). the inertial frames \tilde{z} and z are employed to represent the original (eccentric) and the transformed problems, respectively. According to [8], the planes $\tilde{z} = \tilde{x} + i\tilde{y}$ and $z = x + iy$ are related via

$$z = \tilde{x}_2 \frac{r_1 \tilde{z} - \tilde{x}_1}{\tilde{r}_1 \tilde{z} - \tilde{x}_2}, \quad (1)$$

where

$$\tilde{x}_{1,2} = \tilde{a} \mp (\tilde{a}^2 - \tilde{r}_1^2)^{1/2}, \quad (2)$$

$$\tilde{a} = 1 + (\tilde{r}_1^2 - \tilde{r}_0^2)/L^2, \quad (3)$$

$$\begin{cases} \tilde{x}_1 \tilde{x}_2 = \tilde{r}_1^2 \\ (\tilde{x}_1 - L)(\tilde{x}_2 - L) = \tilde{r}_0^2. \end{cases} \quad (4)$$

Analyzing the above equations, it is possible to verify that, when L increases, \tilde{x}_1 and the inverse of \tilde{x}_2 decreases. Such an important relationship will be useful in the next section where a series solution in terms of \tilde{x}_2^{-1} will be proposed. The electromagnetic parameters of the tilde and non-tilde frames are related by [9]

$$\mathbf{G} = \tilde{\mathbf{J}} \cdot \tilde{\mathbf{G}}, \quad \text{with } \mathbf{G} = \{\mathbf{E}, \mathbf{H}\}, \quad (5)$$

$$\bar{\rho} = |\bar{J}|^{-1} \bar{J} \cdot \bar{\rho} \cdot \bar{J}^T, \quad \text{with } p = \{\varepsilon, \mu\}, \quad (6)$$

where \mathbf{E} and \mathbf{H} are electric and magnetic fields, respectively, $\bar{\varepsilon} = \text{diag}(\bar{\varepsilon}_s, \bar{\varepsilon}_s, \bar{\varepsilon}_z)$ and $\bar{\mu} = \text{diag}(\bar{\mu}_s, \bar{\mu}_s, \bar{\mu}_z)$ are the permittivity and permeability tensors, and \bar{J} is the Jacobian transformation matrix and your determinant can be written by

$$|\bar{J}|^{-1} = \frac{(1 - \tilde{x}_1/\tilde{x}_2)^2}{(1 - 2\rho \cos \phi / \tilde{x}_2 + \rho^2/\tilde{x}_2^2)^2}. \quad (7)$$

Notice that an isotropic and homogeneous eccentric coaxial waveguide is transformed into a concentric guide, but filled with inhomogeneous and anisotropic media in the non-tilde frame, i.e., $\bar{\varepsilon} \rightarrow \bar{\varepsilon}(\rho, \phi)$ and $\bar{\mu} \rightarrow \bar{\mu}(\rho, \phi)$.

2.2 Perturbation Method

Consider now that the transformed concentric-waveguide (in z -plane) has electromagnetic fields that can be seen as a *perturbed* version of those present in a uniaxially-anisotropic and homogeneous waveguide. The latter will be denoted as *unperturbed* fields and identified by the subscript 0. Then, we can write

$$\begin{aligned} \mathbf{E}_0 &= \mathbf{E}_0^+ e^{+ik_{0,z}z} & \mathbf{E} &= \mathbf{E}^- e^{-ik_z z} \\ \mathbf{H}_0 &= \mathbf{H}_0^+ e^{+ik_{0,z}z} & \mathbf{H} &= \mathbf{H}^- e^{-ik_z z}, \end{aligned} \quad (8)$$

where each field have a different propagation direction with respect to the longitudinal axis. Notice we have assumed and omitted the time-harmonic factor $e^{-i\omega t}$. Based in theory of cavity-material perturbation presented in [7], the $k_{0,z}$ and k_z are related via

$$\frac{k_{0,z} - k_z}{\omega} = \frac{\int_S (\Delta \bar{\varepsilon} \cdot \mathbf{E}^- \cdot \mathbf{E}_0^+ + \Delta \bar{\mu} \cdot \mathbf{H}^- \cdot \mathbf{H}_0^+) dS}{\int_S (\mathbf{E}_0^+ \times \mathbf{H}^- + \mathbf{E}^- \times \mathbf{H}_0^+) \cdot \hat{\mathbf{z}} dS}, \quad (9)$$

with $\Delta \bar{\rho} = \bar{\rho} - \bar{\rho}_0$, where $p = \{\varepsilon, \mu\}$.

By assuming the zeroth-order $\bar{\rho}_0$ and perturbed media $\bar{\rho}$ are characterized by

$$\bar{\rho}_0 = \begin{bmatrix} p_s & 0 & 0 \\ 0 & p_s & 0 \\ 0 & 0 & p_{0,z} \end{bmatrix}, \quad \bar{\rho} = \begin{bmatrix} p_s & 0 & 0 \\ 0 & p_s & 0 \\ 0 & 0 & p_z(\rho, \phi) \end{bmatrix}, \quad (10)$$

where $p_z(\rho, \phi)$ can be expanded as a power series in term of \tilde{x}_2^{-1} , namely,

$$\begin{aligned} p_z(\rho, \phi) &= p_{0,z} \left[1 + \frac{4\rho \cos \phi}{\tilde{x}_2} + \frac{2\rho^2}{\tilde{x}_2^2} (3 \cos 2\phi + 2) \right] \\ &+ \mathcal{O}(\tilde{x}_2^{-3}), \end{aligned} \quad (11)$$

with $p_{0,z} = \tilde{p}_z (1 - \tilde{x}_1/\tilde{x}_2)^2$. We can readily simplify $\Delta \bar{\rho}$:

$$\Delta \bar{\rho} = \begin{bmatrix} 0 & 0 & 0 \\ 0 & 0 & 0 \\ 0 & 0 & \Delta p \end{bmatrix}, \quad (12)$$

where

$$\Delta p = p_{0,z} \left[\frac{4\rho \cos \phi}{\tilde{x}_2} + \frac{2\rho^2}{\tilde{x}_2^2} (3 \cos 2\phi + 2) \right]. \quad (13)$$

In order to solve (9), we supposed the perturbation does not significantly modify the field patterns, and we can then assume that the perturbed fields and unperturbed are approximately equal over the plane ρ - ϕ , as long as the eccentricity L is small (or \tilde{x}_2 is large), and consequently, we can write the fields associated to the n th harmonic as

$$\begin{aligned} \mathbf{E}_0^+ &= \mathbf{e}_{np}(\rho) e^{in\phi} & \mathbf{E}^- &= \mathbf{e}_{-np}(\rho) e^{-in\phi} \\ \mathbf{H}_0^+ &= \mathbf{h}_{np}(\rho) e^{in\phi} & \mathbf{H}^- &= -\mathbf{h}_{-np}(\rho) e^{-in\phi}. \end{aligned} \quad (14)$$

Please see [10] for further details. We can now expand the axial wavenumber as a series in \tilde{x}_2^{-1} given by

$$k_z \approx k_{0,z} \left(1 + \frac{\alpha_1}{\tilde{x}_2} + \frac{\alpha_2}{\tilde{x}_2^2} \right), \quad (15)$$

where $k_{0,z}$ is axial wavenumber of the zeroth-order solution, and α_1 and α_2 are the correction factors of first- and second-order, respectively. By combining (14) and (12), and after some manipulations, we simplify the numerator in (9) into two components, one associated with the E -field given by

$$\int_S \Delta \bar{\varepsilon} \cdot \mathbf{E}^- \cdot \mathbf{E}_0^+ dS = \frac{4\varepsilon_{0,z}}{\tilde{x}_2^2} \int_{r_0}^{r_1} e_{z,-np}(\rho) e_{z,np}(\rho) \rho^3 d\rho, \quad (16)$$

and another for the H -field given by

$$\int_S \Delta \bar{\mu} \cdot \mathbf{H}^- \cdot \mathbf{H}_0^+ dS = -\frac{4\mu_{0,z}}{\tilde{x}_2^2} \int_{r_0}^{r_1} h_{z,-np}(\rho) h_{z,np}(\rho) \rho^3 d\rho. \quad (17)$$

Notice that the above equations do not present field components associated with correction of order \tilde{x}_2^{-1} , and as a consequence, we can anticipate that there is no first-order correction in (15), i.e., $\alpha_1 = 0$. The denominator terms in (9) can be obtained via the closed-form resolution of the reaction integrals available in [10]. Finally, by substituting equations (15), (16) and (17) in (9), the corrections α_2 for TE and TM modes can be we can obtained as follows:

$$\alpha_2 = -\frac{\omega}{k_{0,z}} \frac{2\pi}{N_{np}} (I_{TM} + I_{TE}), \quad (18)$$

where

$$N_{np} = \int_S (\mathbf{E}_0^+ \times \mathbf{H}^- + \mathbf{E}^- \times \mathbf{H}_0^+) \cdot \hat{\mathbf{z}} dS, \quad (19a)$$

$$I_{TM} = 4\varepsilon_{0,z} \int_{r_0}^{r_1} e_{z,-np}(\rho) e_{z,np}(\rho) \rho^3 d\rho, \quad (19b)$$

$$I_{TE} = -4\mu_{0,z} \int_{r_0}^{r_1} h_{z,-np}(\rho) h_{z,np}(\rho) \rho^3 d\rho. \quad (19c)$$

3 Numerical Results

In order to validate the presented method, we have first considered the structure of Fig. 1(a), with $\tilde{r}_1 = 5$ mm,

$\tilde{r}_0 = 0.05\tilde{r}_1$, and the eccentricity $L = 0.05\tilde{r}_1$. Table 1 shows the cutoff wavenumbers, given by $k_{\rho c} = (\omega^2 \epsilon_s \mu_s - k_z^2)^{1/2}$, for the dominants TE and TM modes calculated from the finite element method (FEM) in CST Studio Suited [11] and from the method presented in [6] versus those obtained by the our method. The relative error is calculated using the CST results as a reference. The average error of our method (0.263 %) is comparable with the error of the method in [6] (0.264 %).

As a complementary validation, in Fig. 2 we have explored the accuracy of our approach when the latter structure has its eccentricity increased up to 20% of the external radius. Besides that relatively large eccentricity, we can observe that our method remains the accuracy when compared with the full-wave solutions provided by the FEM.

Table 1. Cutoff wavenumbers calculated via FEM (from CST) compared with the results presented in [6] versus our method.

Mode	CST	Our method		Work in [6]	
	$k_{\rho c}$	$k_{\rho c}$	Error (%)	$k_{\rho c}$	Error (%)
TE ₁₁	366.156	367.789	0.446	367.226	0.292
TE ₂₁	610.692	611.333	0.105	612.837	0.351
TE ₃₁	840.159	843.861	0.441	842.354	0.261
TM ₀₁	610.692	614.109	0.559	614.559	0.633
TM ₁₁	775.540	774.695	-0.109	774.038	-0.194
TM ₂₁	1027.331	1028.743	0.137	1029.802	0.241

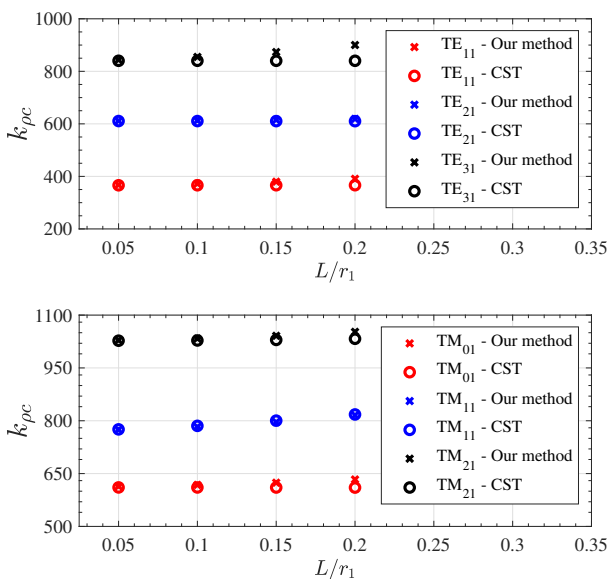


Figure 2. Cutoff wavenumbers for TE (top) and TM (bottom) modes, as a function of the normalized eccentricity L/r_1 , calculated by the FEM (from CST) and by the presented method

4 Conclusion

In this paper, a novel and numerically efficient method to calculate the cutoff wavenumbers (for TE and TM modes) in eccentric coaxial waveguides was developed on the grounds of a conformal mapping combined with a cavity-material perturbation technique. According to the preliminary results, this approach proved to be accurate in the modeling of normalized eccentricity up to 20%. Further work is in progress to improve the presented method for providing additional perturbation correction to the vector fields in addition to the cutoff wavenumbers presented herein.

5 Acknowledgements

This worked was partially supported by Brazilian agency CNPq through the doctoral fellowship number 141617.

References

- [1] H. Y. Yee and N. F. Audeh, "Cutoff frequencies of eccentric waveguides," *IEEE Transactions on Microwave Theory and Techniques*, vol. 14, no. 10, pp. 487–493, 1966.
- [2] J. A. Roumeliotis and J. G. Fikioris, "Cutoff wave numbers of eccentric circular and concentric circular-elliptic metallic wave guides," *Radio Science*, vol. 15, no. 05, pp. 923–937, 1980.
- [3] A. D. Kotsis and J. A. Roumeliotis, "Cutoff wavenumbers of eccentric circular metallic waveguides," *IET Microw., Antennas Propag.*, vol. 8, no. 2, pp. 104–111, Jan. 2014.
- [4] B. N. Das and O. J. Vargheese, "Analysis of dominant and higher order modes for transmission lines using parallel cylinders," *IEEE transactions on microwave theory and techniques*, vol. 42, no. 4, pp. 681–683, 1994.
- [5] J. R. Kuttler, "A new method for calculating te and tm cutoff frequencies of uniform waveguides with lunar or eccentric annular cross section," *IEEE Trans. Microw. Theory Techn.*, vol. 32, no. 4, pp. 348–354, Apr. 1984.
- [6] M. Gholizadeh, M. Baharian, and F. H. Kashani, "A simple analysis for obtaining cutoff wavenumbers of an eccentric circular metallic waveguide in bipolar coordinate system," *IEEE Trans. Microw. Theory Techn.*, vol. 67, no. 3, pp. 837–844, Mar. 2019.
- [7] R. F. Harrington, *Time-Harmonic Electromagnetic Fields*. New York, NY, USA: McGraw-Hill, Chapter 7, 1961.
- [8] H. Kober, *Dictionary of conformal representations*. Dover New York, 1957, vol. 2.

- [9] G. S. Rosa, J. R. Bergmann, F. L. Teixeira, and M. S. Novo, "A perturbation-based method to model electromagnetic logging sensors in eccentric boreholes via conformal transformation optics," in *12th European Conference on Antennas and Propagation (EuCAP 2018)*, Apr. 2018, pp. 1–5.
- [10] G. S. Rosa, "Electromagnetic well-logging tools in complex geophysical formations," Ph.D. dissertation, PUC-Rio, 2017.
- [11] CST AG, CST Studio Suite 2019, Darmstadt, Germany, 2019.